materials

MDPI

Communication

Two New Red/Near-Infrared Ir(III) Complexes with Reversible and Force-Induced Enhanced Mechanoluminescence

Yuzhen Yang, Qin Zeng, Weiqiao Zhou, Junjie Jiang, Zihao Zhang, Song Guo * and Yuanli Liu *

Guangxi Key Laboratory of Optical and Electronic Materials and Devices, College of Materials Science and Engineering, Guilin University of Technology, Guilin 541004, China; yangyuzhen812@163.com (Y.Y.); zqinnn@163.com (Q.Z.); wangyi123zhou@163.com (W.Z.); jiejiangjjj0513@163.com (J.J.); 1020190104@glut.edu.cn (Z.Z.)

* Correspondence: bobingjin@glut.edu.cn (S.G.); lyuanli@glut.edu.cn (Y.L.)

Abstract: Two novel ionic red/near-infrared Ir(III) complexes (Ir1 and Ir2) were reasonably designed and prepared using 2-(1-isoquinolinyl)-9,10-anthraquinone as the main ligand and 4,4′-dimethyl-2,2′-bipyridyl and 4,4′-dimethoxy-2,2′-bipyridyl as the auxiliary ligands, respectively. Both complexes showed bright phosphorescence in solution (peak at 618 nm with a shoulder at 670 nm). Interestingly, the phosphorescence peak of two Ir(III) complexes showed a blue-shift of about 36 nm after being ground. Simultaneously, both complexes exhibited mechanical force-induced enhanced emission, and the intensity of the luminescence for Ir1 and Ir2 increased by around two times compared to the one before being ground, respectively. Powder X-ray diffraction (PXRD) and time-dependent density functional theory (TD-DFT) calculation were utilized to understand well the mechanism of this phenomenon and suggested that the destruction of the well-ordered crystalline nature and the decline in triplet-triplet annihilation maybe responsible for the pressure-induced blue-shift and the enhancement of the phosphorescence.

Keywords: ionic iridium(III) complexes; red/near-infrared phosphorescence; mechanoluminescence; force-induced enhanced emission

check for updates

Citation: Yang, Y.; Zeng, Q.; Zhou, W.; Jiang, J.; Zhang, Z.; Guo, S.; Liu, Y. Two New Red/Near-Infrared Ir(III) Complexes with Reversible and Force-Induced Enhanced Mechanoluminescence. *Materials* **2023**, *16*, 4702. https://doi.org/10.3390/ma16134702

Academic Editor: Heesun Yang

Received: 26 April 2023
Revised: 29 May 2023
Accepted: 5 June 2023
Published: 29 June 2023

Copyright: © 2023 by the authors. Licensee MDPI, Basel, Switzerland. This article is an open access article distributed under the terms and conditions of the Creative Commons Attribution (CC BY) license (https://creativecommons.org/licenses/by/4.0/).

1. Introduction

In recent years, tremendous attention has been given to smart luminescent materials whose photophysical properties can be regulated by various external stimulus (temperature [1,2], light [3,4], force [5], electric field [6,7], magnetic field [8], pH [9], specific ions [10,11], etc.). Upon external stimulus, such as pressure, grinding, and stretching, organic luminogens may exhibit evident changes in emission color and intensity except for chemical reactions, which are called mechanochromic luminescent (MCL) materials [12,13]. These materials could be applied in pressure sensors, optical data recording, and storage devices [14–16].

Mechanochromic luminogens, as captivating materials, have been extensively studied based on numerous pure organic small molecules [17,18], some metal complexes [19,20], liquid crystalline materials [21], and polymers [21]. Tong et al. [22] developed two solution-processable small molecules based on triazatruxene, and the two complexes showed bright blue–green (483 nm) and green (498 nm) emissions, respectively. The emission color of both complexes changed to yellow after being ground in a mortar as the crystalline state changed to amorphous powder. Wang et al. [23] designed and synthesized two asymmetric, traditional β-diketones named TPED2F and TPED2T. TPED2T exhibited a more obvious wavelength shift compared to TPED2F after it was ground and whose maximum emission wavelength showed a red-shift of about 54 nm from 493 nm to 547 nm along with marked color change from cyan to yellow when irradiated with ultraviolet light. Furthermore, TPED2F exhibited reversible mechanochromic properties when being heated, and TPED2T showed irreversible properties when being heated or fumigated. However,

most of the previously reported materials are fluorescent luminogens, and few phosphorescent mechanochromic luminogens were reported. The mechanism of mechanochromic phosphorescent behavior is still unclear, which limits the further exploitation of these materials. Phosphorescent transition-metal complexes, especially Ir(III) complexes, exhibit outstanding photophysical properties, such as abundant triplet excited-state, high luminescence quantum efficiency, and tunable phosphorescence wavelength [24–27], which have been successfully used in the construction of organic light-emitting diodes [28], biosensors [29,30], information encryption [31], optical data recording [32], and storage [33]. Recently, several mechanochromic phosphorescent Ir(III) complexes have been reported. Su [34] and coworkers presented a reversible tricolor (blue, green, and yellow) Ir(III) complex-based luminescent switch, which can be attributed to the transformation from a crystalline state to an amorphous state. In 2021, Zhu [35] and coworkers synthesized two Ir(III) complex isomers, which showed distinctly opposite mechanochromic luminescence despite the same physical phase transformation, and the emitting excited state dominated by triplet charge transfer (^{3}CT) can be responsible for their mechanochromic behaviors. However, the mechanochromic behaviors of most reported Ir(III) complexes are in the range of blue to green or orange, the mechanochromic phosphorescent Ir(III) complexes with red to deep-red emission are extremely rare.

It is well-known that the photophysical properties of the complexes largely rely on the pattern of molecular stacking and the intermolecular interaction in the solid state, and thus, the switch of solid-state luminescence can be achieved by altering molecular arrangement through external stimuli [36–38]. Herein, large conjugated groups, such as anthraquinone and isoquinoline, were introduced into two ionic Ir(III) complexes as main ligands, and 4,4′-dimethyl-2,2′-bipyridine and 4,4′-dimethoxy-2,2′-bipyridyl were selected as auxiliary ligands to prepare red to near-infrared luminogens, respectively. The two complexes showed bright red to near-infrared emission in solution and solid state. Interestingly, the emission spectra of both complexes showed a blue-shift of about 36 nm after being ground. Simultaneously, both complexes exhibited mechanical force-induced enhanced emission. Then, powder X-ray diffraction (PXRD) and time-dependent density functional theory (TD-DFT) calculation were utilized to understand well the mechanism of this phenomenon. The results indicated that the destruction of well-ordered crystalline nature and the decline in triplet-triplet annihilation maybe responsible for the pressure-induced blue-shift and the enhancement of the phosphorescence. We believe that our work will provide a new platform for the future design of highly efficient MCL Ir(III) complexes.

2. Materials and Methods

All reagents and solvents used in this paper were obtained through commercial channels and were used without further purification.

The detailed instrument models are described in Supplementary Materials.

3. Results and Discussion

3.1. Syntheses and Characterization

Two compounds were designed and prepared as shown in Figure 1. First, the main ligand, 2-(1-isoquinolinyl)-9,10-anthraquinone, was synthesized using Suzuki coupling reaction with tetrakis(triphenylphosphine)palladium(0) as a catalyst. Next, dichloro-bridged diiridium complexes and complexes Ir1 and Ir2 were obtained according to the reported methods [39]. The chemical structures of all intermediates and products were confirmed using ^{1}H nuclear magnetic resonance (NMR, 500 MHz), ^{13}C NMR (126 MHz), ^{31}P NMR (201 MHz), ^{19}F NMR (472 MHz) spectra, and matrix-assisted laser desorption ionization time-of-flight mass spectrometry (MALDI-TOF MS). Furthermore, the photophysical properties of the two compounds were investigated using UV–Vis absorption spectrometry, and steady-state and transient phosphorescence spectrometry. From ^{31}P NMR and ^{19}F NMR, it was evident that the coupling constant between the nucleus of ^{31}P and ^{19}F can be calculated

according to the heptet or doublet peak illustrated in the Supplementary Materials. Powder X-ray diffraction (XRD) was utilized to characterize the crystallinity of the two complexes.

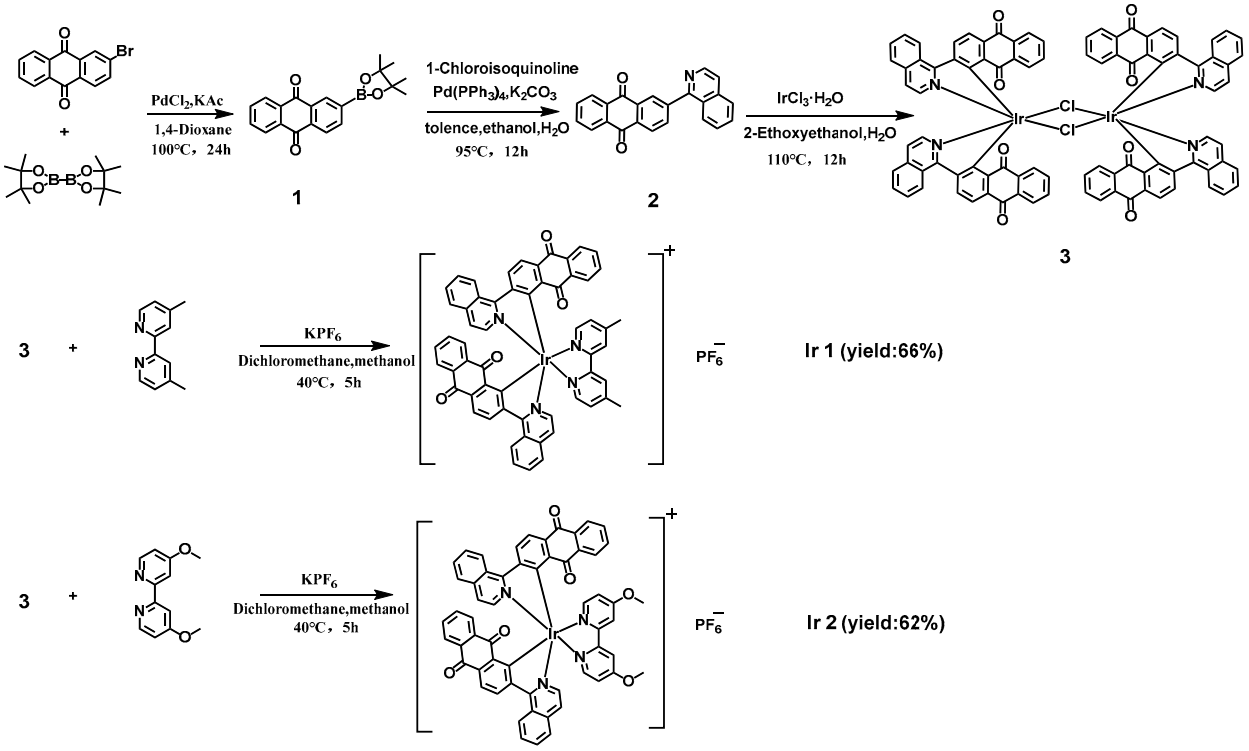


Figure 1. The synthesis of the two complexes.

3.2. Photophysical Properties

First, the photophysical properties of both complexes in solution were investigated. As depicted in Figure 2a, the UV–Vis absorption and emission spectra of Ir1 and Ir2 in dichloromethane (CH_2Cl_2) solution at room temperature were measured, and they exhibited almost the same peak pattern. The strong absorption peak below 315 nm may be attributed to the ligand-centered π-π* transition of 2-(1-isoquinolinyl)-9,10-anthraquinone, and the low-energy absorption band longer than 315 nm may be ascribed to the ^{1}MLCT (metal-to-ligand charge transfer) and ^{1}LLCT (ligand-to-ligand charge transfer) transitions [40].

Then, both complexes (Ir1 and Ir2) exhibited bright red emissions in CH_2Cl_2 solutions visible to the naked eye when excited at 450 nm and their phosphorescence spectra showed a similar profile. For both emissions, full width at half maximum of Ir1 and Ir2 was 60 nm. Next, the emission behaviors of the two complexes in degassed CH_2Cl_2 solution at different concentrations from 1.0×10^{-3} M to 1.0×10^{-5} M were investigated as shown in Figure 2b,c, and the maximum peaks were at about 618 nm. The results revealed that there was almost no or weak intermolecular interaction in dilute solutions.

Moreover, the photoluminescence lifetimes of two complexes in CH_2Cl_2 solutions are listed in Table 1, and the lifetime of Ir2 is obviously shorter than Ir1. The lifetimes of two complexes, Ir1 and Ir2, with peaks at 618 nm were fitted to be 4.58 and 3.55 μs, respectively, and the decay curves (Figure 2g) exhibited single exponential function, demonstrating their triplet-emitting nature. Then, the phosphorescence spectra of the two complexes in various solvents (1,4-dioxane, 2-ethoxyethanol, acetonitrile, CH_2Cl_2, N,N-dimethyl formamide, dimethyl sulfoxide, ethyl acetate, ethanol, methanol, and tetrahydrofuran) with bubbled N_2 are illustrated in Figure 2e,f. It can be clearly observed that the change in the maximum phosphorescence peak of Ir1 and Ir2 is associated with the change in the polarity of the solvent. For instance, the maximum phosphorescence peak for the two complexes in a solution of DMSO (628 nm) and methanol (638 nm) showed a red-shift of

about 10–20 nm compared with that in CH_2Cl_2 (618 nm). The obvious shift suggested that the phosphorescent emission maybe derived from the mixture of LC excited-states and triplet metal-to-ligand charge transfer (^{3}MLCT) [33].

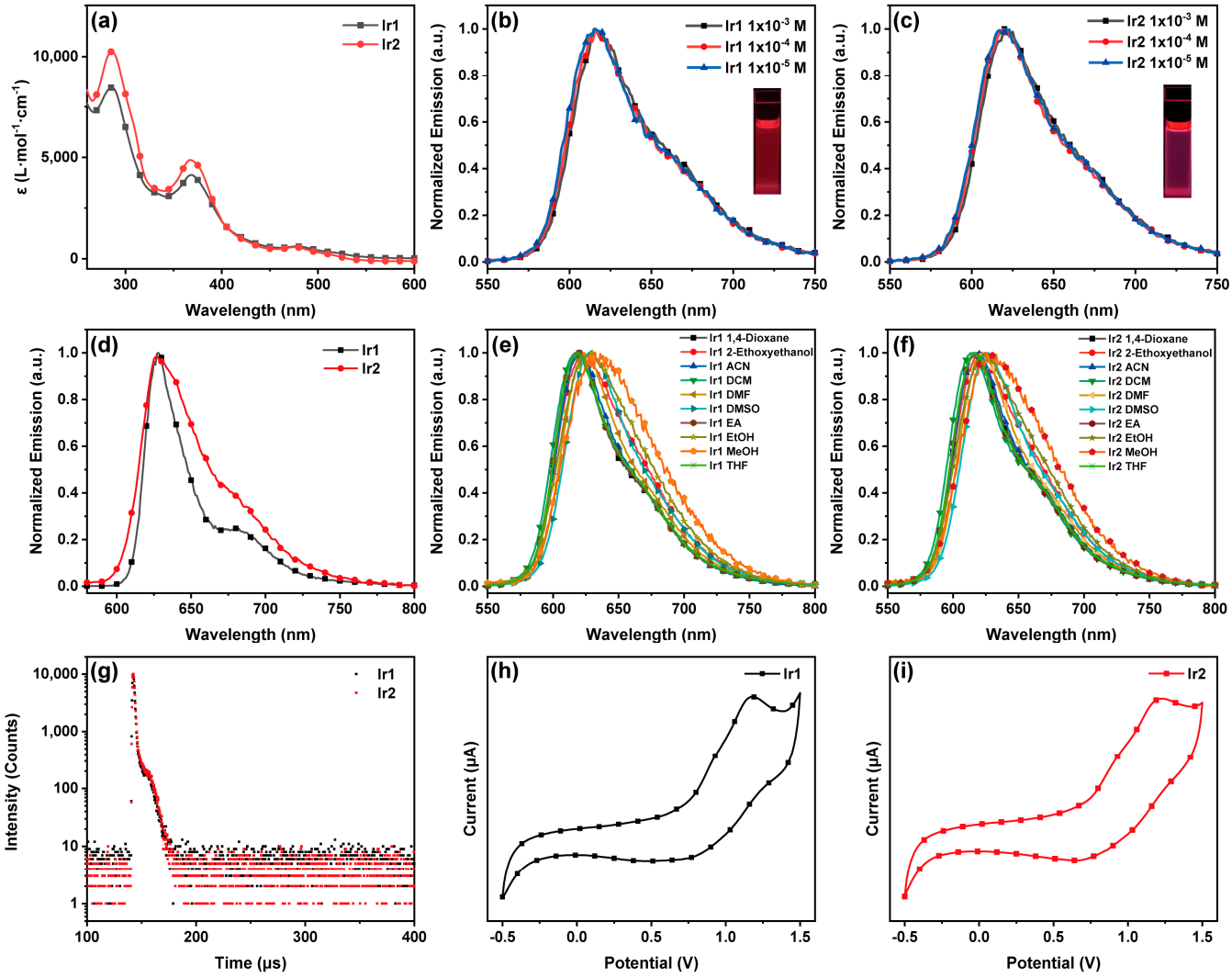


Figure 2. (**a**) Absorption spectra of Ir1 and Ir2 in CH_2Cl_2, (**b**,**c**) phosphorescence spectra of Ir1 and Ir2 at different concentrations in CH_2Cl_2, (**d**) low-temperature phosphorescence spectra (77 K) of Ir1 and Ir2 in CH_2Cl_2, (**e**,**f**) phosphorescence spectra of Ir1 and Ir2 in various solutions (1.0×10^{-5} M), (**g**) the decay curves of the luminescent lifetimes of the two complexes in degassed CH_2Cl_2, (**h**,**i**) cyclic voltammograms of Ir1 and Ir2 under a scan rate of 100 mV/s in CH_2Cl_2.

Table 1. The photophysical data of Ir1 and Ir2.

Complexes	Emission in Degassed CH_2Cl_2		Emission in Solid States		E_g [eV] [a]	E_{onset}^{ox} [eV]	T_1 [eV] [b]
	λ_{em} [nm]	τ [μs]	λ_{em} [nm]	τ [μs]			
Ir1	616	4.58	677	2.21	2.01	0.72	1.97
GIr1	-	-	641	0.94	-	-	-
Ir2	620	3.55	677	1.86	2.00	0.69	1.97
GIr2	-	-	661	0.84	-	-	-

[a] E_g can be calculated from absorption onset according to the UV–Vis spectra. [b] $T_1 = 1240/\lambda_{77K}$.

The low-temperature luminescent spectra of the two complexes in CH_2Cl_2 solutions were measured at 77 K as shown in Figure 2d. The maximum emission peak of Ir1 and Ir2 is at 628 and 627 nm, respectively, showing a slight red-shift compared with that at room temperature, which may result from the increase in the degree of conjugation for the molecules at low temperature. Besides, Ir1 exhibited distinct fine structures of the vibronic band at the peak of 681 nm. The energy level of triplet excited state of Ir1 and Ir2 was calculated to be 1.97 and 1.98 eV, respectively, through the highest-energy vibronic bands from low-temperature luminescent spectra [35].

The electrochemical behaviors of the two complexes were studied using cyclic voltammetry (CV), and the redox potentials are listed in Table 1 and are shown in Figure 2h,i. Ir1 and Ir2 exhibited an irreversible redox process in CH_2Cl_2 solution with oxidation wave at 0.72 V and 0.69 V, respectively, which can be assigned to the oxidation of the Ir center [41,42]. The similar CV curves reveal that different ancillary ligands have a low effect on electrochemical behaviors.

Next, the photophysical properties of Ir1 and Ir2 in solid state and their mechanochromic behaviors were investigated in detail. First, the emission spectra of the two complexes were measured (Figure 3c,f), and the numerical data are summarized in Table 1. The as-synthesized samples and ground samples were named Ir1 and GIr1, respectively (the same as Ir2 and GIr2). Both complexes exhibited deep-red emission visible to the naked eye when excited at 469 nm with the maximum phosphorescence peak at 677 nm. After being ground in a ceramic mortar, complex Ir1 showed a blue-shift from deep-red (λ_{em} = 677 nm) to red (λ_{em} = 641 nm), as depicted in Figure 3a,c. The similar mechanochromic behaviors can be clearly observed for complex Ir2, but Ir2 showed a relatively small force-induced spectral shift (16 nm) compared with Ir1 ($\Delta\lambda_{MCL}$ = 36 nm) (Figure 3b,f). Impressively, two complexes exhibited pressure-induced luminescence enhancement, that is, they are MCL materials. The intensity of the luminescence for Ir1 and Ir2 increased by around two times compared to the one before being ground, respectively. Interestingly, the red luminescence can be easily reverted to near-infrared emission upon fuming with CH_2Cl_2, and the change of emission color in solid states can be repeated several times, suggesting distinguished reversibility in this process (Figure 3e,h). Furthermore, the photoluminescence decay times of Ir1 and Ir2 in solid state before and after being ground were studied, and the luminescent lifetimes of samples in different states were listed as shown in Table 1. It can be clearly seen that the luminescent lifetime (τ) of the as-synthesized sample and ground sample were definitely different, and both of them showed a time-resolved luminescent decay between the two different states. The blue-shift for the two complexes after being ground maybe due to the change of the intermolecular interaction or alteration of the pattern of solid-state molecular packing. π-π interaction between large conjugated groups, such as anthraquinone and isoquinoline, existed in Ir1 and Ir2 and may be weakened after being ground. Furthermore, the pressure-induced luminescence enhancement may result from the decline of the triplet-triplet annihilation before being ground.

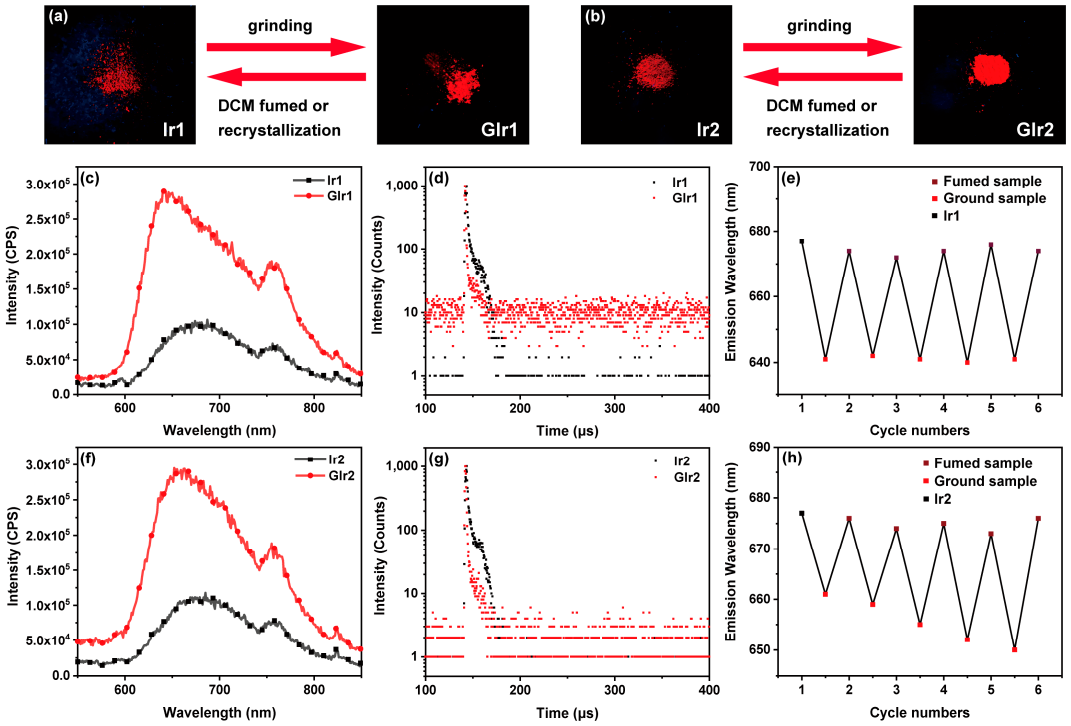


Figure 3. (**a**,**b**) Photographs of Ir1/GIr1 and Ir2/GIr2 upon irradiation with UV light. (**c**,**f**) Emission spectra of complexes Ir1, GIr1, Ir2, and GIr2 in solid states (the emission peak at ca. 750 nm may be caused by the laser). (**d**,**g**) Decay curves of complexes Ir1, GIr1, Ir2, and GIr2 in solid states. (**e**,**h**) Cycles of mechanochromism of Ir1 and Ir2. The letter "G" represents ground samples.

3.3. Mechanochromic Luminescent Mechanism Investigations

In order to realize the possible origin of the MCL behaviors of these two compounds, the powder X-ray diffraction (PXRD) tests were carried out on the as-synthesized sample and ground sample. As illustrated in Figure 4, the intense and sharp reflection peaks can be observed in Ir1 and Ir2, suggesting that these two complexes are well-ordered and crystalline in nature. Moreover, the ground samples showed a weaker diffraction signal, suggesting that the original ordered structures were destroyed. Furthermore, the results showed that the crystallinity of Ir1 is higher than that of Ir2; thus, Ir1 showed an obvious blue-shift compared with Ir2 after being ground. In other words, MCL behaviors of the two iridium(III) complexes may be due to the phase transition from crystalline to amorphous states.

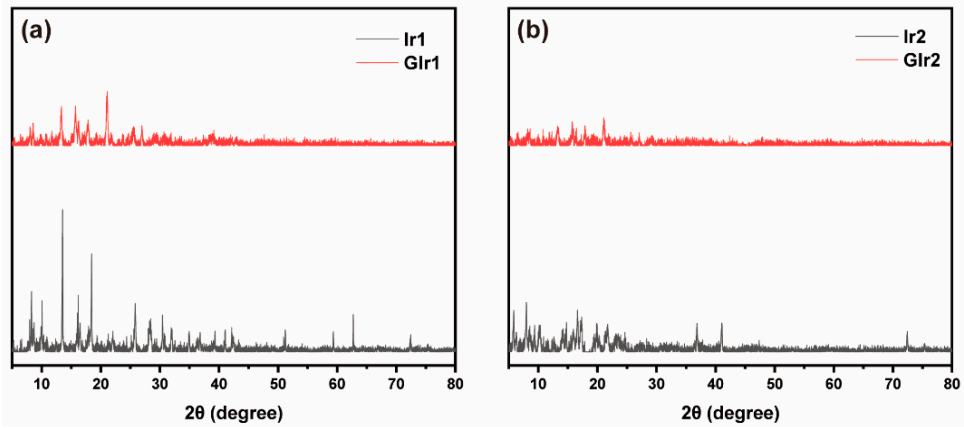


Figure 4. (**a**,**b**) PXRD patterns of as-synthesized sample (Ir1 and Ir2) and ground sample (GIr1 and GIr2).

3.4. Theoretical Calculation

To understand well the underlying mechanism of photophysical properties of the two complexes, theoretical calculation was carried out using B3LYP and time-dependent density functional theory (TD-DFT) (Figure 5 and Table 2). The highest occupied molecular orbital (HOMO) and the lowest unoccupied molecular orbital (LUMO) energy levels of Ir1 and Ir2 are −5.97/−2.98 eV and −5.89/−2.98 eV, respectively. According to the optimized steric configuration, it can be seen that both Ir1 and Ir2 adopted twisted octahedral configuration. The frontier molecular orbitals (FMO) indicated a difference from the common iridium complex. The HOMO and HOMO-1 of the two complexes were located on the main ligand and iridium atom without the ancillary ligands, and the LUMO, LUMO+1, and LUMO+3 of the two complexes were located on the cyclometalating ligand. The triplet excited-states of the two complexes can be assigned to the mixture of MLCT transitions and LLCT transitions. Furthermore, the ancillary ligands were not involved in FMO construction, and this is probably a good explanation for the identical photophysical behaviors of Ir1 and Ir2 [43,44].

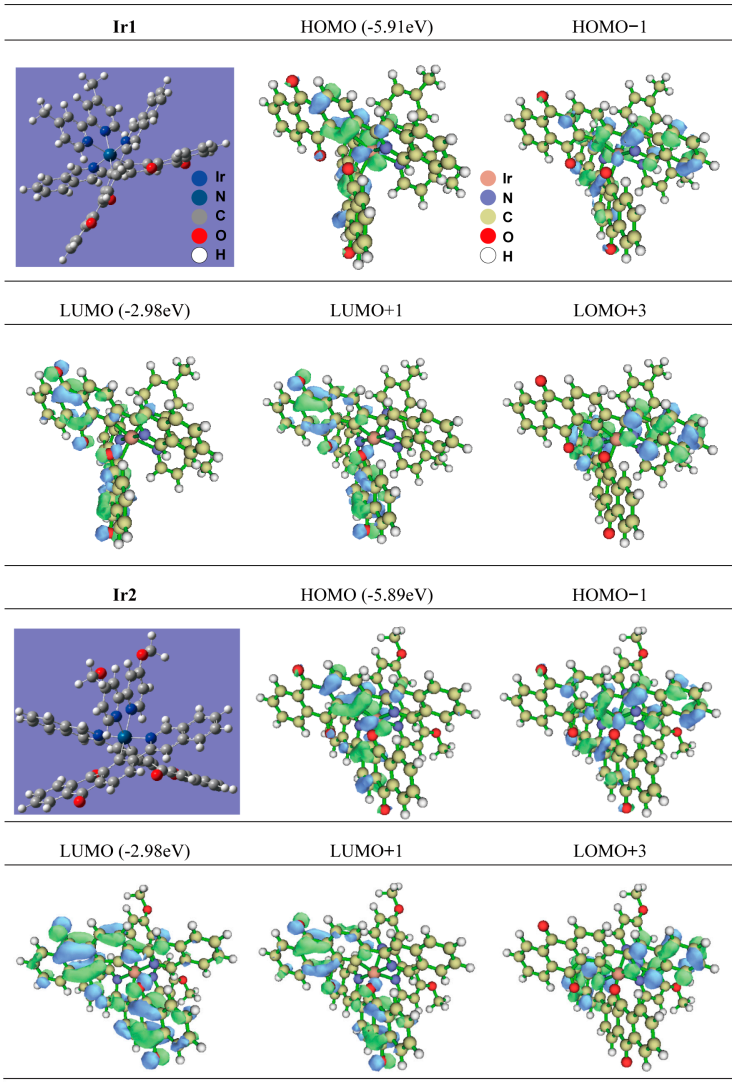


Figure 5. The optimized structures (blue background) and distributions of molecular orbitals (other graphs) of Ir1 and Ir2 (the calculation method is illustrated in the section of calculation method in the Supporting Information).

Table 2. The theoretical calculations of molecular orbital for the two complexes.

Complexes	State	HOMO (eV)	LUMO (eV)	Configuration	Character
Ir1	T_1	−5.97	−2.98	HOMO−1→LUMO+1, 6.48% HOMO−1→LUMO+3, 3.38% HOMO→LUMO, 84.5%	LLCT MLCT/LLCT MLCT/LLCT
Ir2	T_1	−5.89	−2.98	HOMO−1→LUMO+1, 5.78% HOMO−1→LUMO+3, 2.88% HOMO→LUMO, 79.4%	LLCT MLCT/LLCT MLCT/LLCT

4. Conclusions

To sum up, two new cationic iridium(III) complexes with different auxiliary ligands were successfully designed and prepared. Both of them have reversible MCL behaviors, and the emission color can be tuned by grounding and fuming with a solution. Moreover, the MCL properties of Ir1 with methyl-bearing ancillary ligands are more remarkable. The transformation between crystalline and amorphous states and π-π interaction between large conjugated groups maybe the primary reasons for the MCL behavior. In addition, two complexes showed red photoluminescence in the solid and solution state. The different ancillary ligands play a functional role in their MCL behaviors but have a neglectable influence on the photophysical behaviors. We believe that our work will provide valuable guidelines for researchers to design and prepare novel phosphorescent MCL materials based on iridium(III) complexes in the future.

Supplementary Materials: The following supporting information can be downloaded at: https://www.mdpi.com/article/10.3390/ma16134702/s1, Figure S1: The ^{1}H NMR spectrum of the main ligand 2-(1-isoquinolinyl)-9,10-anthraquinone. Figures S2–S6: The NMR spectra and MALDI-TOF spectrum of Ir1. Figures S7–S11: The NMR spectra and MALDI-TOF spectrum of Ir2. Figure S12. PXRD patterns of as-synthesized sample Ir1 and ground sample GIr1. Figure S13. PXRD patterns of as-synthesized sample Ir2 and ground sample GIr2. Reference [45] is cited in the Supplementary Materials.

Author Contributions: Conceptualization, Y.Y., S.G., W.Z. and Q.Z.; methodology, J.J. and S.G.; software, Z.Z. and Y.L.; validation, Y.Y., S.G. and Q.Z.; analysis, Y.Y. and Q.Z.; data curation, S.G., Y.L. and Q.Z.; writing, Y.Y., S.G., W.Z. and Q.Z. All authors have read and agreed to the published version of the manuscript.

Funding: This research was funded by the National Natural Science Foundation of China (21864010) and projects of Guangxi Natural Science Foundation (2020GXNSFBA297098 and 2022GXNSFAA035474).

Institutional Review Board Statement: Not applicable.

Informed Consent Statement: Not applicable.

Data Availability Statement: Raw data are available from the authors upon request.

Conflicts of Interest: The authors declare no conflict of interest.

References

1. Jiang, K.; Wang, Y.; Cai, C.; Lin, H. Conversion of carbon dots from fluorescence to ultralong room-temperature phosphorescence by heating for security applications. *Adv. Mater.* **2018**, *30*, 1800783. [CrossRef] [PubMed]
2. Zhang, N.; Li, J.; Wang, J.; Shi, R.; Chen, L.; Zhang, A.; Yang, P. A vanadate-based white light emitting luminescent material for temperature sensing. *RSC Adv.* **2019**, *9*, 30045–30051. [CrossRef] [PubMed]
3. Huang, G.; Xia, Q.; Huang, W.; Tian, J.; He, Z.; Li, B.S.; Tang, B.Z. Multiple anti-counterfeiting guarantees from a simple tetraphenylethylene derivative—high-contrasted and multi-state mechanochromism and photochromism. *Angew. Chem. Int. Ed.* **2019**, *58*, 17814–17819. [CrossRef] [PubMed]
4. Qi, Q.; Li, C.; Liu, X.; Jiang, S.; Xu, Z.; Lee, R.; Zhu, M.; Xu, B.; Tian, W. Solid-state photoinduced luminescence switch for advanced anticounterfeiting and super-resolution imaging applications. *J. Am. Chem. Soc.* **2017**, *139*, 16036–16039. [CrossRef]

5. Yang, W.; Yang, Y.; Qiu, Y.; Cao, X.; Huang, Z.; Gong, S.; Yang, C. AIE-active multicolor tunable luminogens: Simultaneous mechanochromism and acidochromism with high contrast beyond 100 nm. *Mater. Chem. Front.* **2020**, *4*, 2047–2053. [CrossRef]
6. Sun, H.; Liu, S.; Lin, W.; Zhang, K.Y.; Lv, W.; Huang, X.; Huo, F.; Yang, H.; Jenkins, G.; Zhao, Q.; et al. Smart responsive phosphorescent materials for data recording and security protection. *Nat. Commun.* **2014**, *5*, 3601. [CrossRef]
7. Takeda, Y.; Data, P.; Minakata, S. Alchemy of donor–acceptor–donor multi-photofunctional organic materials: From construction of electron-deficient azaaromatics to exploration of functions. *Chem. Commun.* **2020**, *56*, 8884–8894. [CrossRef]
8. Zhao, Y.; Hou, B.; Liu, C.; Ji, X.; Huang, Y.; Sui, J.; Liu, D.; Wang, N.; Hao, H. Mechanistic study on the effect of magnetic field on the crystallization of organic small molecules. *Ind. Eng. Chem. Res.* **2021**, *60*, 15741–15751. [CrossRef]
9. Cui, J.; Kim, G.; Kim, S.; Kwon, J.E.; Park, S.Y. Ultra-pH-sensitive small molecule probe showing a ratiometric fluorescence color change. *ChemPhotoChem* **2020**, *4*, 393–397. [CrossRef]
10. Huang, W.; Xu, M.; Liu, J.; Wang, J.; Zhu, Y.; Liu, J.; Rong, H.; Zhang, J. Hydrophilic doped quantum dots "ink" and their inkjet-printed patterns for dual mode anticounterfeiting by reversible cation exchange mechanism. *Adv. Funct. Mater.* **2019**, *29*, 1808762. [CrossRef]
11. Long, P.; Feng, Y.; Cao, C.; Li, Y.; Han, J.; Li, S.; Peng, C.; Li, Z.; Feng, W. Self-protective room-temperature phosphorescence of fluorine and nitrogen codoped carbon dots. *Adv. Funct. Mater.* **2018**, *28*, 1800791. [CrossRef]
12. Sagara, Y.; Mutai, T.; Yoshikawa, I.; Araki, K. Material design for piezochromic luminescence: Hydrogen-bond-directed assemblies of a pyrene derivative. *J. Am. Chem. Soc.* **2007**, *129*, 1520–1521. [CrossRef] [PubMed]
13. Yoon, S.-J.; Chung, J.W.; Gierschner, J.; Kim, K.S.; Choi, M.-G.; Kim, D.; Park, S.Y. Multistimuli two-color luminescence switching via different slip-stacking of highly fluorescent molecular sheets. *J. Am. Chem. Soc.* **2010**, *132*, 13675–13683. [CrossRef] [PubMed]
14. Zhang, Q.; Yue, S.; Sun, H.; Wang, X.; Hao, X.; An, S. Nondestructive up-conversion readout in Er/Yb co-doped Na0.5Bi2.5Nb2O9-based optical storage materials for optical data storage device applications. *J. Mater. Chem. C* **2017**, *5*, 3838–3847. [CrossRef]
15. Luo, J.; Li, L.-Y.; Song, Y.; Pei, J. A piezochromic luminescent complex: Mechanical force induced patterning with a high contrast ratio. *Chem.—Eur. J.* **2011**, *17*, 10515–10519. [CrossRef] [PubMed]
16. Zhang, M.; Li, Y.; Gao, K.; Li, Z.; Liu, Y.; Liao, Y.; Duan, Y.; Han, T. A turn-on mechanochromic luminescent material serving as pressure sensor and rewritable optical data storage. *Dye. Pigment.* **2020**, *173*, 107928. [CrossRef]
17. Liu, Z.; Liu, Y.; Qi, F.; Yan, H.; Jiang, Z.; Chen, Y. Flexible π-conjugated 2,5-diarylamino-terephthalates: A new class of mechanochromic luminophores with tunable aggregation states. *Chem. A Eur. J.* **2020**, *26*, 14963–14968. [CrossRef]
18. Dong, Y.; Zhang, J.; Tan, X.; Wang, L.; Chen, J.; Li, B.; Ye, L.; Xu, B.; Zou, B.; Tian, W. Multi-stimuli responsive fluorescence switching: The reversible piezochromism and protonation effect of a divinylanthracene derivative. *J. Mater. Chem. C* **2013**, *1*, 7554–7559. [CrossRef]
19. Zhu, S.; Hu, J.; Zhai, S.; Wang, Y.; Xu, Z.; Liu, R.; Zhu, H. AIPE-active Pt(II) complexes with a tunable triplet excited state: Design, mechanochromism and application in anti-counterfeiting. *Inorg. Chem. Front.* **2020**, *7*, 4677–4686. [CrossRef]
20. Han, Y.; Cao, H.-T.; Sun, H.-Z.; Wu, Y.; Shan, G.-G.; Su, Z.-M.; Hou, X.-G.; Liao, Y. Effect of alkyl chain length on piezochromic luminescence of iridium(III)-based phosphors adopting 2-phenyl-1H-benzoimidazole type ligands. *J. Mater. Chem. C* **2014**, *2*, 7648–7655. [CrossRef]
21. Manbeck, G.F.; Brennessel, W.W.; Stockland, R.A., Jr.; Eisenberg, R. Luminescent Au(I)/Cu(I) alkynyl clusters with an ethynyl steroid and related aliphatic ligands: An octanuclear Au_4Cu_4 cluster and luminescence polymorphism in Au_3Cu_2 clusters. *J. Am. Chem. Soc.* **2010**, *132*, 12307–12318. [CrossRef] [PubMed]
22. Han, X.; Tong, J.; Ding, G.; Sun, C.; Wang, X.; Su, Z.; Sun, J.; Wen, L.-L.; Shan, G.-G. Highly emissive coordination polymer derived from tetraphenylethylene-tetrazole chromophore: Synthesis, characterization and piezochromic luminescent behavior. *Chin. Chem. Lett.* **2023**, *34*, 107255. [CrossRef]
23. Liu, W.; Wang, Y.; Yang, J.; Li, X.; Wang, X.; Ma, L. The abnormal solvatochromism, high-contrast mechanochromism and internal mechanism of two AIEE-active β-diketones. *Dye. Pigment.* **2020**, *175*, 108149. [CrossRef]
24. Costa, R.D.; Ortí, E.; Bolink, H.J.; Monti, F.; Accorsi, G.; Armaroli, N. Luminescent ionic transition-metal complexes for light-emitting electrochemical cells. *Angew. Chem. Int. Ed.* **2012**, *51*, 8178–8211. [CrossRef]
25. Ulbricht, C.; Beyer, B.; Friebe, C.; Winter, A.; Schubert, U.S. Recent developments in the application of phosphorescent iridium(III) complex systems. *Adv. Mater.* **2009**, *21*, 4418–4441. [CrossRef]
26. Chi, Y.; Chou, P.-T. Transition-metal phosphors with cyclometalating ligands: Fundamentals and applications. *Chem. Soc. Rev.* **2010**, *39*, 638–655. [CrossRef]
27. Tao, P.; Lü, X.; Zhou, G.; Wong, W.-Y. Asymmetric tris-heteroleptic cyclometalated phosphorescent iridium(III) complexes: An emerging class of metallophosphors. *Acc. Mater. Res.* **2022**, *3*, 830–842. [CrossRef]
28. Su, N.; Li, S.; Yang, K.; Zhou, F.; Song, J.; Zhou, L.; Qu, J. High efficiency electroluminescence of orange-red iridium(III) complexes for OLEDs with an EQE over 30%. *Dye. Pigment.* **2021**, *195*, 109733. [CrossRef]
29. Yu, Y.; Wu, Y.; Liu, J.; Liu, Y.; Wu, D. Highly efficient dual-modal phosphorescence/computed tomography bioprobes based on an iridium complex and AuNP polyiohexol composite nanoparticles. *Nanoscale* **2017**, *9*, 9447–9456. [CrossRef]
30. Tao, P.; Lv, Z.; Zheng, X.-K.; Jiang, H.; Liu, S.; Wang, H.; Wong, W.-Y.; Zhao, Q. Isomer engineering of lepidine-based iridophosphors for far-red hypoxia imaging and photodynamic therapy. *Inorg. Chem.* **2022**, *61*, 17703–17712. [CrossRef]
31. Song, Z.; Liu, R.; Zhu, H.; Lu, Y.; Li, X.; Zhu, H. Smart inks based on AIPE-active heteroleptic Ir(III) complexes. *Sens. Actuators B Chem.* **2019**, *279*, 385–392. [CrossRef]

32. Orselli, E.; Kottas, G.S.; Konradsson, A.E.; Coppo, P.; Fröhlich, R.; De Cola, L.; van Dijken, A.; Büchel, M.; Börner, H. Blue-emitting iridium complexes with substituted 1,2,4-triazole ligands: Synthesis, photophysics, and devices. *Inorg. Chem.* **2007**, *46*, 11082–11093. [CrossRef] [PubMed]
33. Yang, B.; Tao, P.; Ma, C.; Tang, R.; Gong, T.; Liu, S.; Zhao, Q. Iridium(iii) complex-containing non-conjugated polymers for non-volatile memory induced by switchable through-space charge transfer. *J. Mater. Chem. C* **2020**, *8*, 5449–5455. [CrossRef]
34. Yang, T.; Wang, Y.; Liu, X.; Li, G.; Che, W.; Zhu, D.; Su, Z.; Bryce, M.R. Reversible tricolour luminescence switching based on a piezochromic iridium(III) complex. *Chem. Commun.* **2019**, *55*, 14582–14585. [CrossRef] [PubMed]
35. Li, G.; Yang, T.; Shao, K.; Gao, Y.; Shan, G.; Su, Z.; Wang, X.; Zhu, D. Understanding mechanochromic luminescence on account of molecular level based on phosphorescent iridium(III) complex isomers. *Inorg. Chem.* **2021**, *60*, 3741–3748. [CrossRef] [PubMed]
36. Tsukuda, T.; Kawase, M.; Dairiki, A.; Matsumoto, K.; Tsubomura, T. Brilliant reversible luminescent mechanochromism of silver(I) complexes containing o-bis(diphenylphosphino)benzene and phosphinesulfide. *Chem. Commun.* **2010**, *46*, 1905–1907. [CrossRef]
37. Balch, A.L. Dynamic crystals: Visually detected mechanochemical changes in the luminescence of gold and other transition-metal complexes. *Angew. Chem. Int. Ed.* **2009**, *48*, 2641–2644. [CrossRef]
38. Wang, Y.; Li, M.; Zhang, Y.; Yang, J.; Zhu, S.; Sheng, L.; Wang, X.; Yang, B.; Zhang, S.X.-A. Stress acidulated amphoteric molecules and mechanochromism via reversible intermolecular proton transfer. *Chem. Commun.* **2013**, *49*, 6587–6589. [CrossRef]
39. Nonoyama, M. Benzo[h]quinolin-10-yl-n iridium(III) complexes. *Bull. Chem. Soc. Jpn.* **1974**, *47*, 767–768. [CrossRef]
40. Jing, Y.; Wang, F.; Zheng, Y.; Zuo, J. Efficient deep red electroluminescence of iridium(III) complexes with 2,3-diphenylquinoxaline derivatives and tetraphenylimidodiphosphinate. *J. Mater. Chem. C* **2017**, *5*, 3714–3724. [CrossRef]
41. Guo, C.; Guo, S.; Lu, Q.; Jiang, Z.; Yang, Y.; Zhou, W.; Zeng, Q.; Liang, J.; Miao, Y.; Liu, Y. Solution-processed yellow organic light-emitting diodes based on two new ionic Ir (III) complexes. *Molecules* **2022**, *27*, 2840. [CrossRef] [PubMed]
42. Lu, Z.; Lu, Q.; Yang, Y.; Jiang, Z.; Zeng, Q.; Zhou, W.; Jun, L.; Gong, Y.; Liu, Y.; Miao, Y.; et al. Solution-processed high-performance orange-red organic light-emitting diode (OLED) based on ionic phosphorescent iridium(III) complex. *J. Organomet. Chem.* **2022**, *967*, 122333. [CrossRef]
43. Lu, T.; Chen, F. Multiwfn: A multifunctional wavefunction analyzer. *J. Comput. Chem.* **2012**, *33*, 580–592. [CrossRef] [PubMed]
44. Frisch, M.; Trucks, G.; Schlegel, H.; Scuseria, G.; Robb, M.; Cheeseman, J.; Scalmani, G.; Barone, V.; Petersson, G.; Nakatsuji, H. *Gaussian 16 Revision c. 01*; Gaussian Inc.: Wallingford, CT, USA, 2016; 421.
45. Tao, P.; Li, W.L.; Zhang, J.; Guo, S.; Zhao, Q.; Wang, H.; Wei, B.; Liu, S.J.; Zhou, X.H.; Yu, Q.; et al. Facile synthesis of highly efficient lepidine-based phosphorescent iridium(III) complexes for yellow and white organic light-emitting diodes. *Adv. Funct. Mater.* **2016**, *26*, 881. [CrossRef]

Disclaimer/Publisher's Note: The statements, opinions and data contained in all publications are solely those of the individual author(s) and contributor(s) and not of MDPI and/or the editor(s). MDPI and/or the editor(s) disclaim responsibility for any injury to people or property resulting from any ideas, methods, instructions or products referred to in the content.